EXPERIMENTAL STUDY ON SEISMIC BEHAVIOR OF INTEGRAL ABUTMENT-PILE-SOIL UNDER LOW-CYCLE PSEUDO-STATIC TEST

Fuyun Huang(1), Feng Zhang(2), Wei Chen(3)

(1) *Professor, College of Civil Engineering, Fuzhou University, huangfuyun@fzu.edu.cn*
(2) *Postgraduate, College of Civil Engineering, Fuzhou University, 2576967333@qq.com*
(3) *Postgraduate, College of Civil Engineering, Fuzhou University,1306701509@qq.com*

Abstract

The integral abutment jointless bridge (IAJB) has a long service life, convenient construction, less building and maintenance costs. In currently, it has been widely used and applied. However, interaction of pile-soil of IAJB would be performed under the seasonal temperature load or seismic excitation. Therefore, based on a practical IAJB in China, the abutment-pile structural test model was designed and manufactured, and the reciprocating low-cycle pseudo-static test on interaction of integral abutment-H-shaped pile-soil was carried out. The hysteretic behavior, lateral deformation law and the interactive mechanism of integral abutment-pile-soil were studied. The testing results indicate that the equivalent damping ratio of abutment and pile is more than 0.15, which means the IAJB has a favorable seismic performance. The pile of IAJB is in elastic stage under the temperature effect, but it has a residual deformation. The reasons of bumping at bridge end and the settlement under approach slap not only relate to the backfill properties of abutment, but also relate to the mechanism behavior of abutment-structure-soil. In addition, only measured and analyzed the deformation over surface of pile cannot accurately demonstrate the distribution of lateral deformation of embedded pile. The accumulative deformation of abutment-pile-soil interaction is observed, which is significantly larger than that under anyone load step. At present, the existing calculation theory of lateral deformation of abutment-pile foundation does not take into account the impact of accumulative deformation, thus the discovery can be presented as a reference for the relevant codes.

Keywords: IAJB, H-shaped steel pile , abutment-pile-soil, interaction, seismic behavior

1. Introduction

Due to frequent earthquake disasters, bridges are always prone to damage which leads to huge economic losses and even personal casualties. The integral abutment jointless bridge (IAJB) eliminates the expansion joints to consolidate the main girder, abutment and piles as a whole, which greatly reduces the seismic response of the bridge. The IAJB is deemed to own the excellent seismic performance in medium and small span girder bridges[1].

At present, a lot of researches have been carried out to investigate the seismic performance of IAJB. Considering the soil-structure interaction, Wilson[2], Mylonkis[3], Spyrakos[4] and Zhao[5] applied numerical simulation and finite element analysis to explore the dynamic characteristics of IAJB. Goel[6]

monitored a concrete bridge in California for many years, and found that the period and damping of the structure can be significantly increased by the backfill.

However, few research works about the experiments on the seismic performance of integral abutment-steel H-pile-soil of IAJB[7-9]. Therefore, this paper intends to carry out pseudo-static test research on the interaction of integral abutment, H-shaped steel pile and soil under the action of horizontal forces such as temperature. Due to space limitation, this paper only gives hysteretic curve, skeleton curve, model displacement and abutment rotation angle, and analyses displacement accumulative deformation law of abutment-pile foundation model specimens. In this paper, the movement of abutment toward the soil behind abutment (bank slope direction) is called positive direction, and the movement of abutment away from the soil behind abutment (river span direction) is called negative direction.

2. Experimental design

2.1 Design and construction of specimen

The design and fabrication of model specimen in this experiment is the same as those in references[7-8]. The geometric scale ratio of the specimen is selected to be 0.31.The abutment has a length of 0.56m, width of 0.66m and height of 1m. The steel H-pile at bottom of abutment with strong axial width of 0.217m, weak axial width of 0.155m, total length of 3.21m, slenderness ratio of 20.7, flange thickness of 10mm and web thickness of 6mm, as shown in figure 1.The design parameters and casting of model specimens are listed in detail in the reference[7].

2.2 Soil container and soil

In this experiment, the size of the soil box of 2m×3m×4m was selected, as shown in figure 2. The detail information of the soil box and the filling method of soil are available in the paper[7]. The test soil is taken from Min-jiang River, Fuzhou. The average penetration number of model sand is 11 by standard penetration test, which belongs to slightly dense sand.

Fig.1: Specimen

Fig.2: Testing apparatus

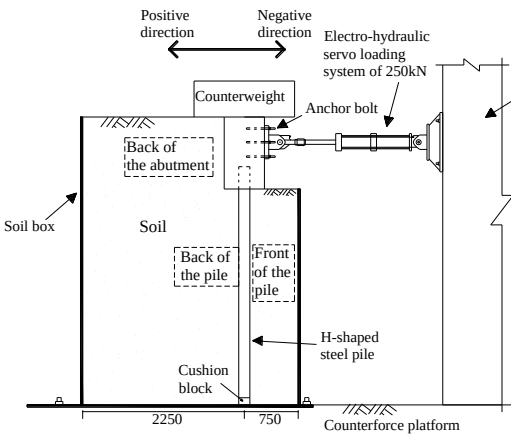

Fig.3: Loading arrangement

2.3 Loading device and scheme

Four types of sensors were used in the experiment: earth pressure cell, displacement gauge, inclinometer and strain gauge. The MTS electro-hydraulic servo loading system was used to simulate the displacement and deformation of the main girder under seismic load by applying low cyclic horizontal displacement load at the abutment. The MTS actuator was connected with the screw embedded in the abutment at 0.35m below the top of abutment, the loading arrangement was shown in Figure 3. The specific loading scheme was designed as follows: (1)initial stage: increment loading with 2mm until 20mm; (2)stages of 20mm to 60mm with increment of 5mm; (3)after 60mm, the increment loading with 10mm,and the test were terminated when the lateral force decreased to 85% of the peak value. The speed of loading in test was 1.0mm/s and each load grad had 3 cycles.

3. Experiment results

3.1 Hysteretic curve

The following definitions of direction of loading force produced by the actuator, are defined when the abutment moves in the positive direction as the horizontal thrust, while the force produced by the actuator when the abutment moves in the negative direction as the horizontal tension. At the same time, the deformation corresponding to the force of 0 kN is defined as residual deformation; when the loading displacement is defined as 0 mm, the horizontal deformation of the model deviates from its central axis is defined as cumulative deformation.

3.1.1 Hysteresis curve

Fig. 4 shows the hysteretic behavior curve of abutment-H-shaped steel pile-soil interaction, in which quadrant 1 represents the hysteretic curve of abutment-pile-soil interaction under positive displacement, quadrant 3 represents the process of abutment-pile-soil interaction under negative displacement, quadrant 2 represents the process of pile-soil interaction transforming into the process of abutment-pile-soil interaction, and quadrant 4 represents the process of abutment-pile-soil interaction. The interaction process is transformed into the pile-soil interaction process. In addition, for the convenience of analysis, only the hysteretic envelope curve under the second action of 14mm displacement load is given, as shown in Fig. 4(b).

When the abutment moves towards the soil(road embankment), the direction is defined as positive; when the abutment moves towards the actuator(bridge),the direction is defined as negative. Figure 4 shows the hysteretic curves for the entire test process, it can be seen that the hysteretic curves are plump and spindle-shaped in the first quadrant. Owing to the existence of backfill behind the abutment, the area in the hysteretic curve formed by the abutment-soil is relatively large, but they are asymmetrical and not spindle-shaped in other three quadrants. The area of the hysteretic curve is obviously smaller than the area of the first quadrant hysteretic curve under the same displacement load. Under positive loading, there are not only has the interaction of pile and soil, but also the interaction of abutment and backfill.And, only the interaction of pile and soil under the negative loading, so the area of the hysteretic curve under the negative loading is much smaller than that under the positive loading. In other word, the energy consumed under the positive loading is much larger than that under negative loading.

It also can be seen from Figure 4 that when the actuator goes back to the initial position. When the actuator force reduces to 0 kN (Point A), the displacement don't be restored to 0 mm. Since the soil is a plastic material, the force-displacement curve is nonlinear during unloading, which leads to the residual deformation. When the displacement returns to 0mm (Point B), the horizontal force of the model is not 0kN resulting from the unbalanced force. For imposing displacement 12mm,30mm,60mm and 90mm, the residual deformation reached 8.07mm, 18.7mm, 36.16mm and 44.04 mm, and the unbalanced force are 16.10kN, 24.11kN, 49.39 kN and 37.77kN for abutment backs to initial position (Point B). Therefore, as the displacement increases, the residual deformation gradually augments, and the unbalanced force enhances before the structure yields but reduces to some extent after the structure yields.

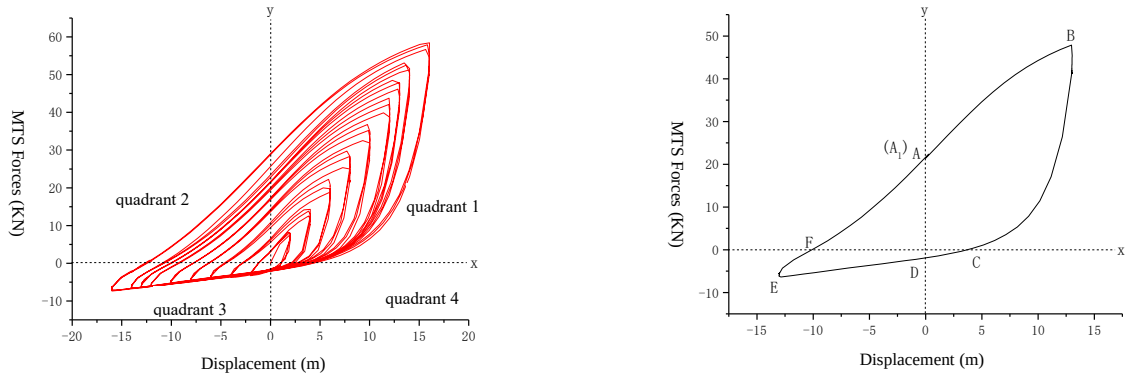

Fig.4: Hysteretic curves for the entire process

Fig. 4(a) shows that the hysteretic curve is full and spindle-shaped, but its hysteretic curve is asymmetrically distributed along the XY axis (displacement symmetry, stress asymmetry). Generally, the hysteretic curves of structures such as piers, piles and columns are usually symmetrical in the axial direction [28,29]. However, the hysteretic curves obtained in this experiment are quite different from those of these structures. When the displacement of abutment is the same in both positive and negative directions, the area surrounded by the hysteretic curve of quadrant 1 and the XY axis is larger than that of quadrant 3. Usually, the area surrounded by hysteretic curve represents the energy dissipation capacity of the structure. Therefore, the energy dissipation capacity of the abutment-pile-soil interaction is greater when the abutment displaces in the positive direction than when the abutment displaces in the negative direction. The area enclosed by the hysteretic curve of quadrant 2 and the XY axis is larger than that of quadrant 3. That is to say, the energy absorbed by the interaction between abutment and soil is larger than that absorbed by the interaction between pile and soil when the bridge shrinks.

Fig. 4(b) shows that when the model is in situ 0 mm, the initial load of point A is 21.51 kN, and then displacement load (AB segment) is applied. As the displacement load of the abutment increases from 0 mm to + 14 mm, that is, point B, the retaining effect of the soil behind the abutment is gradually strengthened, that is, the MTS loading thrust. The thrust increases from 21.51 kN to 47.83 kN.

When the abutment begins to move in the negative direction (BD section), the MTS loading thrust is

gradually unloaded to 0 kN, that is, point C. From point C, it can be seen that the model does not return to 0 mm in situ, because the soil is plastic material, so the force is not a linear change (BC curve) during unloading, resulting in the occurrence of residual deformation, which is about 3.80 mm. In order to classify the model as 0 mm in situ, that is, point D, MTS actuator exerts reverse horizontal tension on the abutment, the size of which is 2.11 kN.

When the displacement loading (DE segment) is continued, the model moves from 0 mm in situ (D point) to -14 mm (E point) in a negative direction. At this time, the horizontal tension exerted by MTS on the abutment reaches 6.29 kN. The DE segment indicates that the abutment moves in a negative direction. In practical engineering, due to temperature drop, shrinkage deformation of main girder and impact of automobile wheel, the abutment moves towards the river span direction (negative direction), and the abutment hardly provides resistance. At this time, the soil behind the abutment will also be affected by vehicle load on the upper part of the abutment, weight of the abutment and self-weight stress of the soil. Following the abutment moving towards the river span direction and filling the gap generated by the abutment, or the soil behind the abutment pushing the abutment moving towards the river span direction, the soil behind the abutment occurs the phenomenon of void subsidence, as shown in the schematic diagram of void subsidence of the soil behind the abutment Fig. 5a~c. Similarly, the change process and void phenomenon were observed in the experiment, as shown in Fig. 5d. Therefore, besides the characteristics of the soil behind the abutment, the reasons for the bump at the bridge head and the settlement behind the abutment are also related to the force mechanism of the abutment structure itself.

In addition, except the void subsidence of abutment, void phenomena also occur at the junction area of abutment bottom and pile top, forming a small number of void areas, as shown in Fig. 5c. The reason is that the void occurs when the pile body pushes the soil around the pile foundation under the action of horizontal reciprocating force, and the upper part of the interface is the abutment, not sand, which can not fill the void area in time, thus forming the void phenomenon. However, because the earth pressure behind the abutment is relatively large, most of the void areas will be filled under the action of self-weight, so only a small number of void areas will be generated in the boundary area between the bottom of the abutment and the top of the pile.

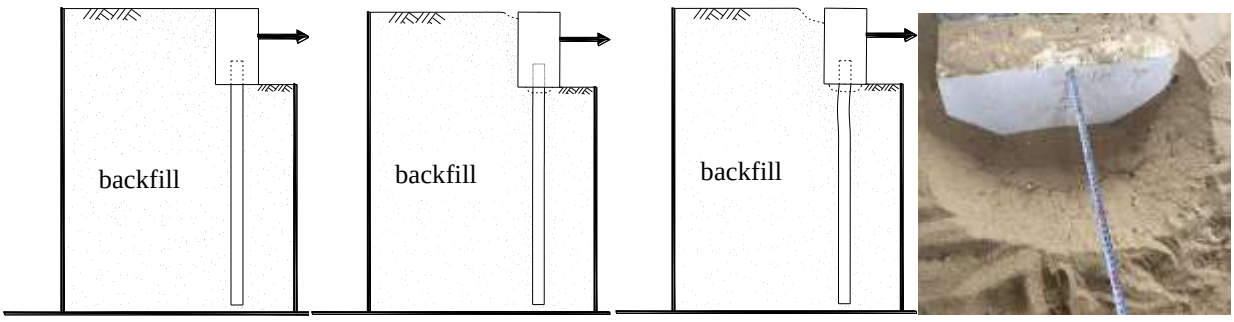

(a) 0mm (b) ±8mm (c) ±14mm (d) Soil void and subsidence

Fig.5 The Settlement of Abutment Backfill and Void

3.1.2 Energy consumption analysis

When the structure is subjected to earthquake, its energy dissipation capacity determines its seismic

performance. Domestic and foreign scholars use equivalent viscous damping ratio, energy dissipation coefficient, power ratio coefficient, normalized energy coefficient to evaluate the energy dissipation capacity of the structure.

It is the equivalent viscous damping ratio curve of the integral abutment and pile foundation under different displacement loads. The larger the equivalent viscous damper ζ_e is, the stronger the energy dissipation capacity of the structure is, and the better the seismic performance of the structure system is. The calculation formula is as follows:

$$\xi_e = \frac{S}{2\pi\left(S_{\triangle 1} + S_{\triangle 2}\right)} \tag{1}$$

In formula: S is the area of hysteresis loop. $S_{\triangle 1}$ is the area enclosed by the displacement axis and the peak point of forward loading. $S_{\triangle 2}$ is the area surrounded by the displacement axis and the peak point of negative loading. It shows that when the displacement load is 0 mm ~ 8 mm, the equivalent viscous damping ratio of abutment increases with the increase of displacement, and is 0.191 under 2 mm displacement. When the displacement load is 8 mm ~ 16 mm, the equivalent viscous damping ratio of abutment tends to be stable gradually, that is, the energy absorbed by the interaction between abutment and soil after 8 mm displacement is stable. And it reached the maximum at 8mm, which was 0.25. The equivalent viscous damping ratio of pile foundation has little change, which is about 0.17. The energy dissipation effect of integral abutment-pile foundation-soil is better and has better seismic performance.

In addition, by comparing the equivalent viscous damping ratio of abutment and pile foundation, it can be seen that the equivalent viscous damping ratio of abutment is larger than that of pile foundation, and the maximum ratio of the two can reach 1.43 times. That is to say, the seismic capacity of the IAJB is mainly provided by the interaction between the abutment and soil, or the energy dissipation capacity of the abutment is much greater than that of the pile-soil.

3.2 Model horizontal deformation distribution

3.2.1 Curve of relationship between horizontal deformation

Fig. 6 shows the relationship between the horizontal deformation of abutment and pile body along the depth direction under the action of positive displacement loads. From the graph, the displacement of abutment decreases linearly from the top to the bottom of abutment, so the displacement of abutment can be regarded as a rigid body displacement with a certain rotation angle.

For the horizontal deformation of pile body, it is obviously different from the traditional theoretical calculation results of pile foundation. As can be seen from Fig. 6, the displacement at the top of the pile is not the largest. When the displacement load is 0 mm to 12 mm, and the depth of the pile in the soil is within 0 m to 0.2 m, the displacement of the pile increases rapidly along the depth of the soil, and the horizontal deformation reaches the maximum at the depth of 0.2 m (1.29B). In the range of 0.2m~0.9m, the displacement of pile body gradually decreases with the increase of the depth of soil entry. At the depth of 0.9m (5.8B), the displacement of pile body decreases to 0 mm and begins to be negative. At the depth of 1.2m (7.74B), the horizontal displacement of pile body reaches the maximum negative value, and thereafter (the depth of soil is 1.4m~2.9m), the negative displacement of pile body moves along the depth of soil entry.

The depth increases and gradually decreases to zero. When the displacement load is 14 mm to 16 mm, the horizontal deformation of the pile body is the largest at the depth of 0.4 m (2.58B).

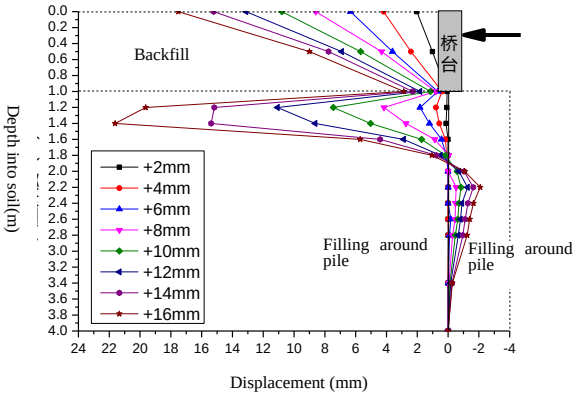

Fig.6 Deformation Curve of Abutment under Displacement Load in Positive Direction

In addition, it can be seen from Fig. 6 that the maximum horizontal deformation of pile body reaches 11.09 mm when the loading displacement is +12 mm, which is close to the loading displacement. When the displacement load continues to increase to +14 mm and +16 mm, the maximum horizontal deformation of pile body reaches 15.33 mm and 21.64 mm, and the maximum horizontal deformation even exceeds the loading displacement.

For the horizontal deformation of pile body, it can be seen from Fig. 6 that the value is basically negative, and gradually decreases with the increase of the depth of soil entry. However, when the loading displacement is -6mm and -8mm, the displacement of pile body changes abruptly at the depth of 0.2m (1.29B), and the horizontal deformation of pile body hardly increases. It can be seen from Fig. 6 that when the displacement load increases to -10mm, the horizontal deformation of the buried depth further decreases, and is less than -4mm ~ -8mm displacement load (as shown in the dashed line of Fig. 6). In addition, when the displacement load continues to increase, the horizontal deformation at this point decreases rapidly to 0 mm and begins to reverse sharply to positive value. If the displacement load is -16mm, the maximum horizontal deformation of the point reaches +11.83mm.

From the flow path of the soil in Fig. 5, it can be seen that when the model moves in the positive direction, the soil around the pile (bank side) under the platform is squeezed by the pile body, but the soil in front of the pile (river side) is void and forms voids. Because the earth pressure of the soil behind the pile (bank side) is squeezed by the level and rotation of the upper abutment, the earth pressure behind the pile is much larger than that of the front side of the pile. Therefore, the soil behind the abutment and the soil behind the pile will flow to the front side of the pile and fill the void, instead of being usually filled by the soil at the front side of the pile, so that the pile body will appear to the side of the bank slope. The deformation is cumulative deformation.

When the abutment moves in the negative direction, although the pile body deforms in the negative direction, the accumulated deformation value even exceeds the deformation caused by this displacement loading because of the large accumulated deformation. For example, when the displacement of -16mm is loaded, the accumulated deformation at D9 point reaches 15.85mm, and the actual deformation under this loading step is only -4.02mm. Therefore, the measured horizontal deformation at D9 point is +11.83mm.

3.2.2 Displacement change history

In order to analyze and discuss the horizontal deformation law of pile body along the depth direction in detail, the horizontal deformation histories of each test point of abutment-pile-soil interaction model specimens are given in Fig. 7, as shown in Fig. 7. Limited to space, this paper only gives the horizontal deformation history diagrams of several key points on the model, as shown in Fig. 7b to Fig. 7j. They are model D14 (located at the top of the abutment), D13, D11 (at the bottom or top of the abutment), D10, D9, D8, D7, D5 and D2 (1.8m below the top of the pile, that is 11.61B). For ease of understanding, Fig. 7a shows the layout of each measuring point and the sketch of the geometric center axis deviation after the cumulative deformation of the model under the action of displacement load.

For abutment, the change of its horizontal deformation history is consistent with the displacement loading history , and is also basically symmetrical with the time axis, which indicates that the soil behind abutment has little influence on it, or that only measuring the deformation of the upper unfilled structure can not accurately reflect the deformation law of the whole structure. However, due to the rotation of abutment, the horizontal deformation at D14 is slightly larger than the loading displacement. From Fig. 7c, it can be seen that the deformation of D13 point is less than the displacement of loading point, and there is a more obvious downward deviation from the time axis, indicating that the soil behind the abutment has a certain impact on its deformation. For example, when the loading displacement is 16 mm, the center axis is about -2.19 mm downward, and the downward displacement indicates that the center axis has a negative deformation (far from the bank slope). The offset value is the cumulative deformation of the center axle of abutment under various reciprocating loads, as shown in the dashed line of Fig. 7c-h. Similarly, D11 point (abutment bottom) also produces downward migration. For example, under 16 mm displacement loading, accumulated deformation at D11 point is about -3.92 mm. The main causes of cumulative deformation are shown in section 3.1 and Fig. 5. The cumulative deformation far from the bank slope (or moving towards the river span) is also one of the mechanical mechanisms and causes of soil void and subsidence and vehicle bump at the bridge abutment.

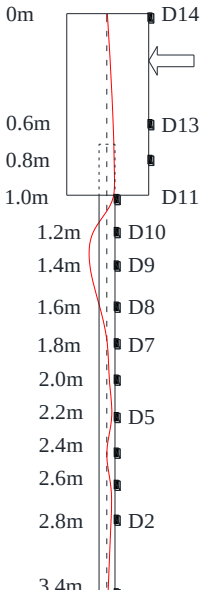

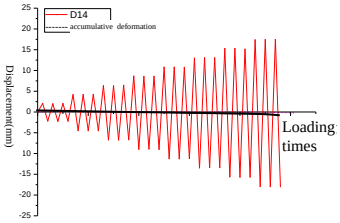

(b) D14 Displacement history

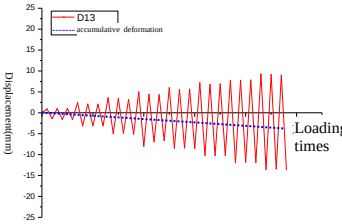

(c) D13 Displacement history

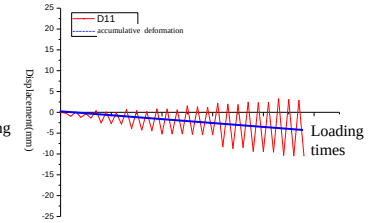

(d) D11Displacement history

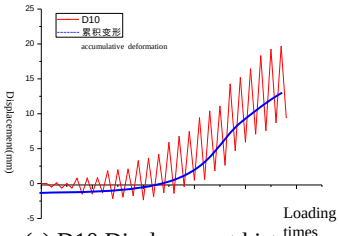

(e) D10 Displacement history

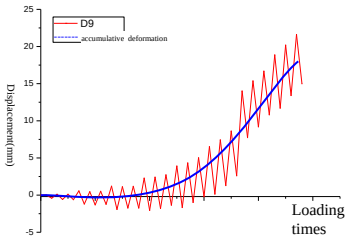

(f) D9 Displacement history

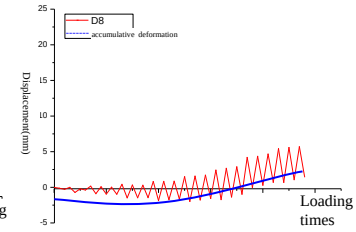

(g) D8 Displacement history

(a) Displacement meter layout

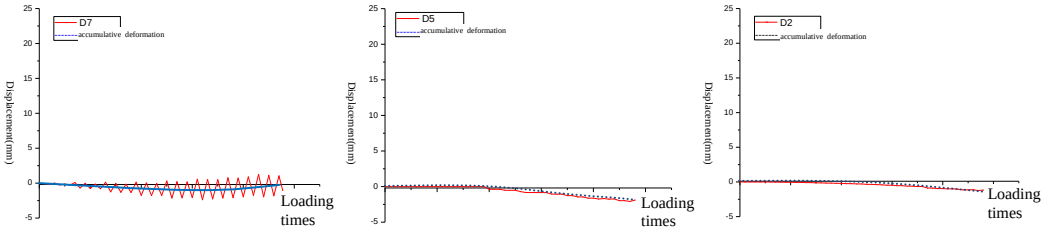

(h) D7 Displacement history (i) D5 Displacement history (j) D2 Displacement history

Fig.7 Horizontal Deformation Process of Measured Points in the Model

For the pile body, it can be seen from Fig. 7e that a large cumulative deformation occurs at D10 point. When the loading displacement is +16 mm, the maximum cumulative deformation reaches 14.0 mm. However, when the displacement load is less than 6 mm, there is no accumulated deformation, and when the displacement load exceeds 6 mm, the accumulated deformation increases rapidly. It shows that the cumulative deformation of abutment can be neglected when the force of abutment is small. The reasons for the accumulated deformation of pile body are basically similar to those of abutment. When the abutment is loaded reciprocally, the pile foundation under the abutment is pushing the soil around the pile, which results in voids at the top of the pile and within a certain depth and width of the pile. When the void occurs, because the earth pressure behind the abutment is greater than that before the pile, the void in front of the pile is filled and compacted continuously by the soil behind the abutment, which eventually leads to the cumulative deformation of the model behind the abutment. That is to say, the deformation process is no longer symmetrical along the time axis (or the original geometric center axis of the model), but begins to change off-axis at a certain time of movement, which is called the accumulation of deformation. Among them, D10-D8 points show positive cumulative deformation and D7-D2 points show negative cumulative deformation. The positive cumulative deformation at D9 point is the largest, reaching +16.77 mm, and the negative cumulative deformation at D11 point is the largest, reaching -3.92 mm.

3.2.3 Deformation under one-step displacement load

The so-called deformation under one-step displacement load refers to the asymmetrical deformation along the center of the model under this step load after the cumulative deformation is deducted. In order to analyze and discuss the law of horizontal deformation of pile body along the depth direction under single-step displacement load, the horizontal deformation history of each test point of abutment-pile-soil interaction model specimens under single-step displacement load is given in Fig.8. The horizontal deformation histories of several key points in the model are given, as shown in Fig. 8b to Fig. 8j. Meanwhile, for ease of understanding, Fig. 8a gives the layout of each measuring point and the schematic diagram of the deformation (the central axis) under the single-step displacement load of +16mm.

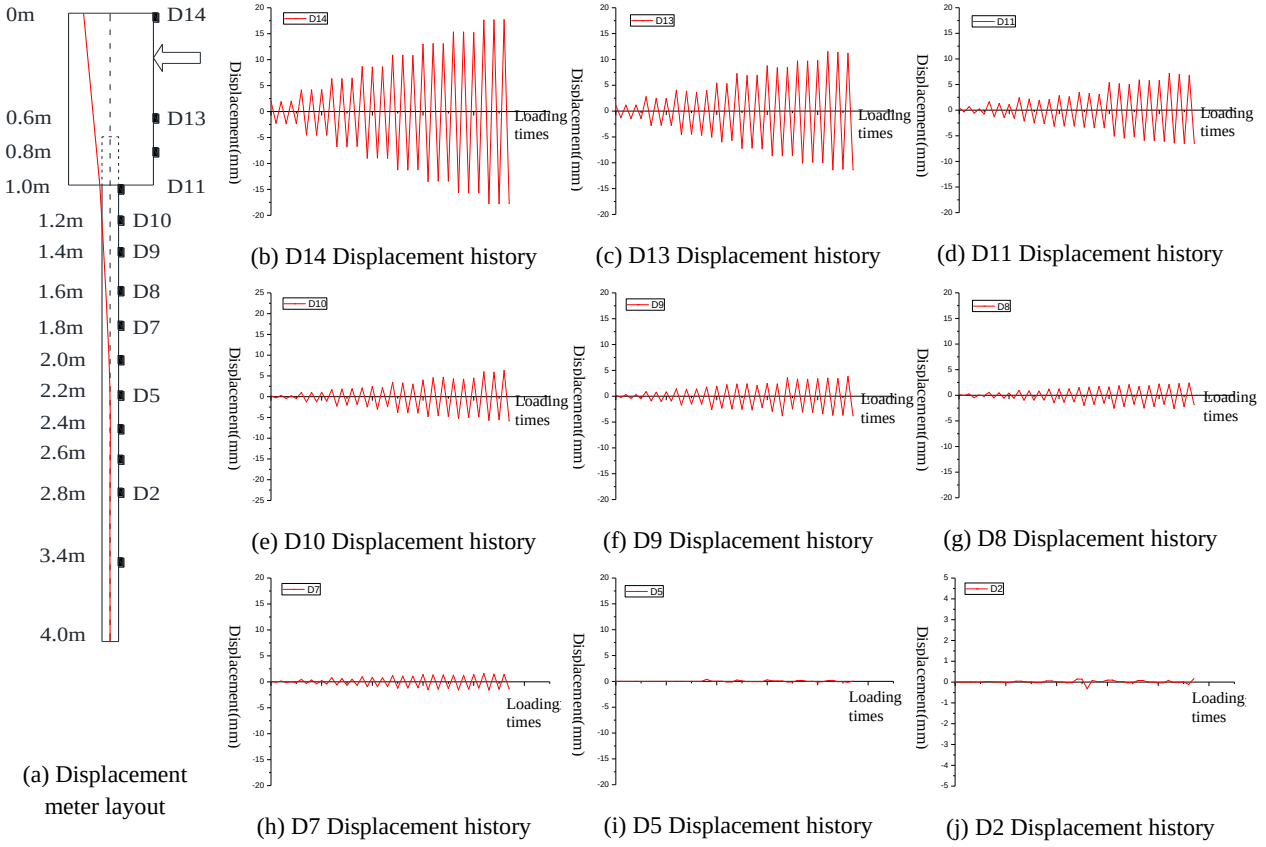

(a) Displacement meter layout

(b) D14 Displacement history

(c) D13 Displacement history

(d) D11 Displacement history

(e) D10 Displacement history

(f) D9 Displacement history

(g) D8 Displacement history

(h) D7 Displacement history

(i) D5 Displacement history

(j) D2 Displacement history

Fig.8 Horizontal Deformation Process under Single Step Displacement Load

For abutments, it can be seen from Fig. 8b and Fig. 8c that the change of horizontal deformation history under single-step displacement load is basically consistent with the displacement loading history, which is asymmetrical with time. Under the action of +16mm single-step displacement load, the horizontal deformation at D14 point is 17.66mm, while the offer at D13 point is less than the displacement at loading point, which is 11.35mm. Compared with Fig. 7, the cumulative deformation of abutment is obviously smaller than that under single-step displacement load. Similarly, the horizontal deformation process of D11 under single-step displacement load is similar to that of D13. For example, the horizontal deformation of D11 under single-step displacement load is +6.70 mm and -6.63 mm.

For the pile body, from Fig. 8e to Fig. 8j, it can be seen that the horizontal deformation caused by any single-step displacement load is small and smaller than that at the top (bottom) of the pile. For example, the horizontal deformations at D9, D8 and D7 points are +3.50 mm, +2.21 mm and +1.37 mm respectively under the action of +16 mm single-step displacement load, which are significantly less than the +6.70 mm at D11 points. However, the horizontal deformation in the deeper area, including the pile bottom, is negligible. For example, the horizontal deformation at the embedment depth of 2.8m (D2 point) is only 0.1mm under the action of 16mm displacement load, but the cumulative deformation reaches 2.0mm. Compared with Fig. 7 and Fig. 8, the cumulative deformation of pile body is much larger than that under arbitrary single-step displacement load. Therefore, the horizontal deformation of model piles obtained by theoretical calculation in practical engineering is mainly under single-step load. If the cumulative deformation of model structure is not taken into account, the results will be deviated greatly.

3.3 Abutment angle

Fig. 9 shows the angle-displacement curve of abutment. It can be seen from the graph that when the abutment moves in both positive and negative directions, its rotation angle increases linearly with the increase of loading displacement. When the displacement load is 0 mm ~ 6 mm, the positive and negative abutment rotation angles are almost equal, and the influence of backfill on abutment rotation angle can be neglected. When the displacement load is 6 mm ~ 16 mm, the positive abutment rotation angle is larger than the negative one, and the difference between them increases gradually. When the displacement load is 16 mm, the maximum positive rotation angle is 0.75 degrees, while the maximum negative rotation angle is 0.51 degrees. The reason is that the abutment is easy to move in the negative direction and difficult to rotate (so the rotation angle is small), while the earth pressure behind the abutment makes the abutment difficult to move in the positive direction and easy to rotate. It shows that the filling behind the abutment has a certain influence on the abutment angle, that is, the angle of the abutment under the heating action is 1.47 times that under the cooling action. However, in general, the abutment angle is not large, all less than 1° .

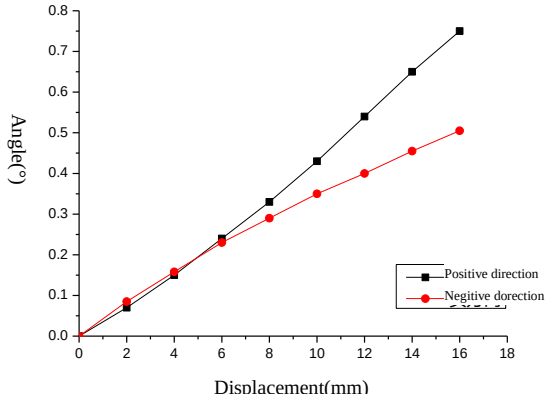

Fig.9 Abutment Angle-displacement Curves

4. Conclusion

In this paper, low-cycle reciprocating pseudo-static tests of abutment-pile-soil interaction are carried out. The hysteretic behavior, deformation law and interaction mechanism of abutment-pile-soil are studied. The following conclusions are drawn:

(1) The skeleton curves of the model specimens during the loading process are all within the linear elastic range, which indicates that this type of abutment and H-shaped steel pile foundation can better withstand the expansion and contraction deformation of the main girder under the action of temperature.

(2) The shape of the abutment-pile foundation-soil hysteretic curve is full and shows shuttle shape. The equivalent viscous damping ratio of the abutment and pile foundation is larger than 0.15, and the abutment is larger than the pile foundation. It shows that this type of bridge has good seismic performance and energy dissipation capacity. However, the hysteretic curves of model specimens are different from those of general structures or pile foundations in morphology, mainly with large residual deformation. The residual deformation of the river side is larger than that of the bank side. The larger the loading displacement, the larger the residual deformation. The residual deformation of the river side can reach 72% of the loading displacement.

(3) The test results show that the horizontal thrust of the MTS actuator increases gradually with the

increase of the number of cycles. The maximum horizontal thrust of the MTS actuator under the same stage load can increase by 13.1%. There will be void phenomenon in a certain width and depth range between abutment back and pile top under reciprocating loading. The results show that the causes of bumping at the bridge head and the settlement of the slab are related not only to the characteristics of the soil behind the abutment, but also to the mechanical mechanism of the abutment structure.

(4) The research shows that the accumulative deformation of abutment-pile foundation will occur under low-cycle reciprocating load. The accumulative deformation of pile foundation is larger than that of abutment, and the accumulative deformation is much larger than that under arbitrary single-step load. Only measuring and analyzing the deformation of the upper structure without soil can not accurately reflect the deformation law of the whole structure. Therefore, the effect of accumulated deformation should be considered in practical engineering.

(5) Although the cumulative deformation of H-shaped steel piles in integral bridges has been found in this paper, only a single test has been carried out at present, and there is still a lack of parametric analysis of finite element method. Therefore, the author will further verify the cumulative deformation of steel piles in the later period.

5. Acknowledgement

The work is financially supported by the National Natural Science Foundation of China (No.51578161).

6. References

[1] Chen B C,Zhuang Y Z,Bruno B (2013): Jointless Bridges. Beijing :*China Communications Press*.(in Chinese)

[2] Wilson J C,Tan B S.(1990).Bridge Abutments: Formulation of Simple Model for Earthquake Response Analysis.*Journal of Engineering Mechanics*, **116**(8):1828-1837.

[3] Mylonakis G, Papastamatiou D, Psycharis J, et al.(2001).Simplified Modeling of Bridge Response on Soft Soil to Nonuniform Seismic Excitation.*Journal of Bridge Engineering*, **6**(6): 587-597.

[4] Spyrakos C,Loannidis G.(2003).Seismic Behavior of a Post-Tensioned Integral Bridge Including Soil-Structure Interaction. *Soil Dynamics and Earthquake Engineering*, **23**(1):53-63.

[5] Vasheghani F R, Q Zhao, Burdette E G.(2010).Seismic Analysis of Integral Abutment Bridges in Tennessee,Including Soil-Structure Interaction.Transportation Research Record:*Journal of the Transportation Research Board*, **2201**(1): 70-79.

[6] Goel R K.(1997).Earthquake Characteristics of Bridges with Integral Abutments.*Journal of Structure Engineering*, **123**(11):1435-1443.

[7] Huang F Y,Lin Y W,Cheng J F,et al.(2019).Interaction of Integral Abutment-H-shaped Steel Pile-soil Under Reciprocating Low-cycle Pseudo-static Test.*China Journal of Highway and Transport*, **32**(05):100-114.(in Chinese)

[8] Huang F Y, Cheng J F,Xue J Q,et al.(2019). Experimental Study on the Interaction of Abutment-Pile-Soil with Expanded Polystyrenes of Integral Abutment Jointless Bridges.*China Journal of Highway and Transport*, **32**(07):77-89.(in Chinese).(in Chinese)

[9] Huang F Y,Zhuag Y Z,Fu C,et al. (2015).Review on Seismic Performance and Simplified Design Method of Jointless Bridge.*Earthquake Engineering and Engineering Dynamics*, **35(**5):15-22.(in Chinese)